



Material considerations for third generation photon detectors

A. Rogalski

Institute of Applied Physics, Military University of Technology
2 Kaliskiego St., 00-908 Warsaw, Poland

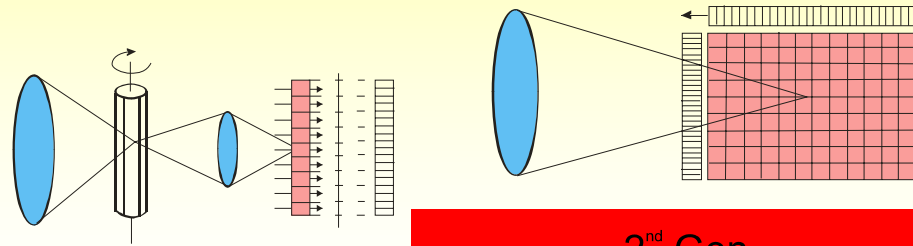
rogan@wat.edu.pl



Outline

- Introduction
- Requirements of third generation infrared systems
- HgCdTe photodiodes and QWIP for third generation detectors
- InAs/GaInSb as a promising material system for third generation detectors
 - Material properties
 - Superlattice photodiodes
 - Focal plane arrays
- Conclusions

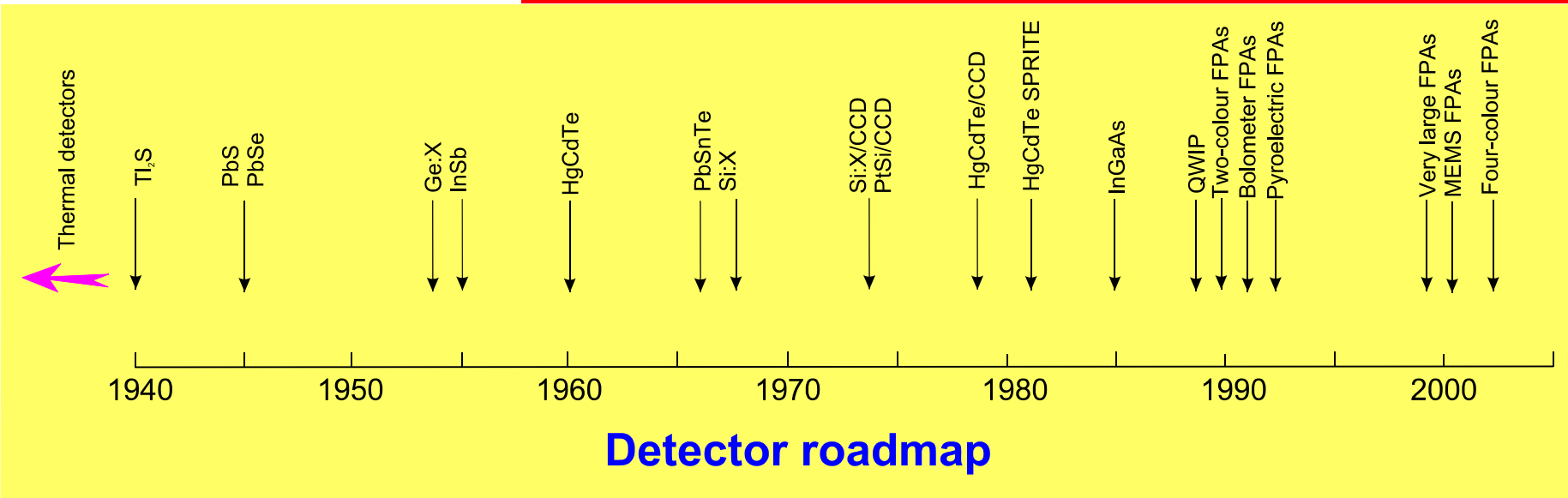
Detector roadmap



1st Gen, Scan to image

2nd Gen
FPA+ROIC

3rd Gen
FPA+ROIC





Third generation IR systems

Third generation IR systems provide enhanced capabilities like:

- larger number of pixels,
- higher frame rates,
- better thermal resolution,
- multicolour functionality and other on-chip functions.

3rd Gen. devices includes [D. Reago *et al.*, *Proc. SPIE 3701*, 108–117 (1999)]:

- high performance, high resolution cooled imagers having two- or three-colour bands,
- medium- to high-performance uncooled imagers,
- very low cost, expendable uncooled imagers.

Development of third generation photon systems has been possible due to impressive progress in the growth of epitaxial layers



Noise equivalent temperature difference (NEDT)

$$NEDT = \left(\tau C \eta_{BLIP} \sqrt{N_w} \right)^{-1}$$

where:

τ is the optics transmission spectrum

C is the thermal contrast

N_w is the number of photogenerated carriers integrated for one integration time t_{int} ,

Q_B is the photon flux density incident on detector area A_d

$$N_w = \eta A_d t_{int} Q_B$$

The *NEDT* is inversely proportional to the square root of the integrated charge and therefore the greater the charge, the higher the performance

2nd Gen imagers provide *NEDT* of about 20–30 mK with f/2 optics.

A goal of 3rd Gen imagers is to achieve sensitivity improvement corresponding to *NEDT* of about 1 mK. Then for a 300 K scene in LWIR region with thermal contrast of 0.02, the required charge storage capacity is above 10^9 electrons.

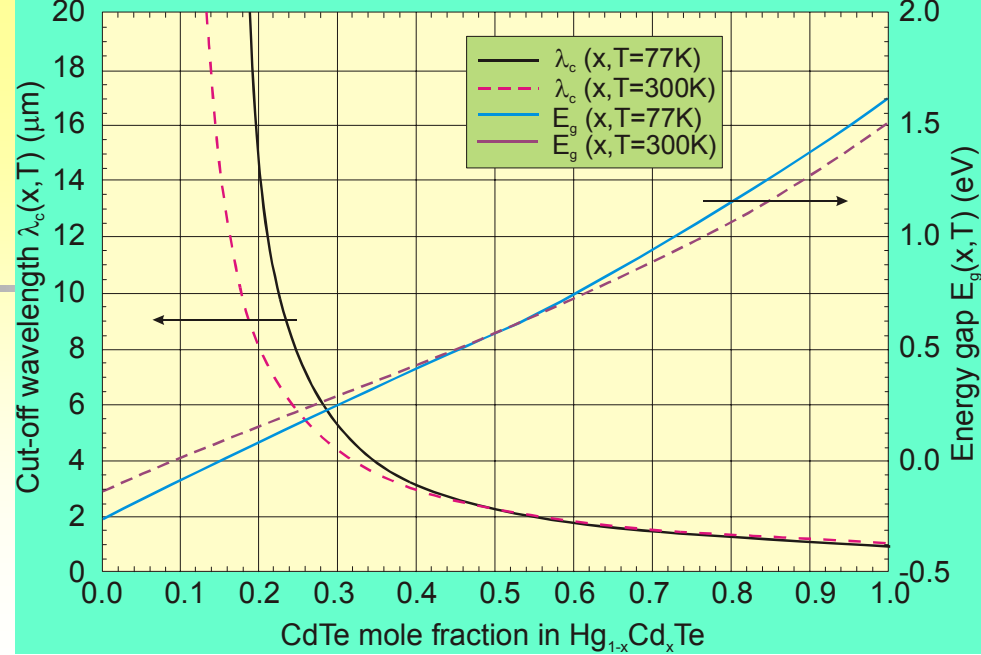
To provide an opportunity to significantly increase both the charge storage capacity and the dynamic range, the VISA program has been sponsored by DARPA

Uniformity

In the LWIR band:

scene contrast $\approx 2\%/K$,

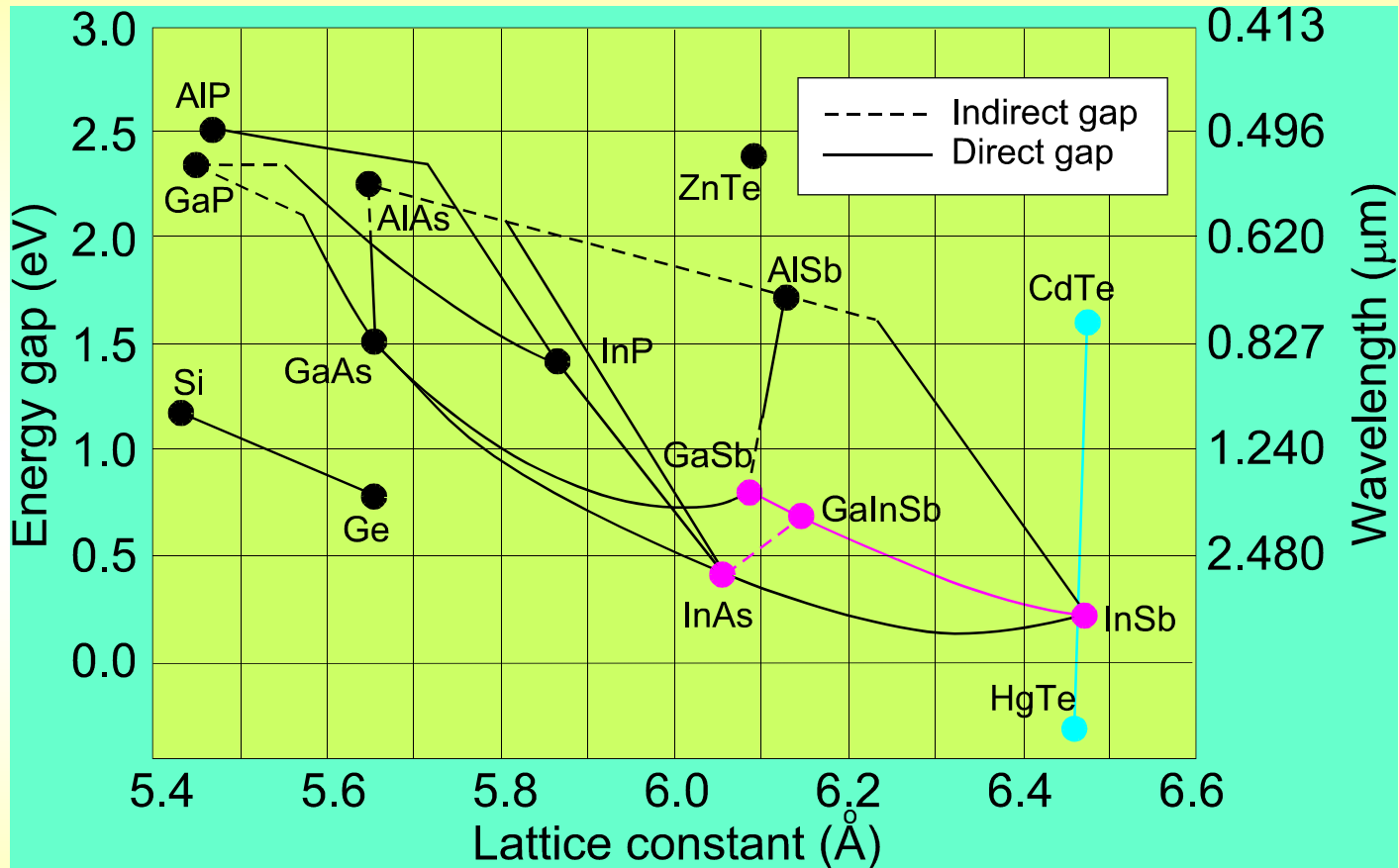
for $NEDT=20$ mK, nonuniformity $< 0.04\%$



Cutoff wavelength vs composition of $\text{Hg}_{1-x}\text{Cd}_x\text{Te}$

Cutoff wavelength for x variations of 0.1%,
and the corresponding cutoff wavelength shift for $\text{Hg}_{1-x}\text{Cd}_x\text{Te}$

x-value	Cutoff wavelength (μm)	Temperature (K)	Uncertainty (μm)
0.395	3	77	0.012
0.295	5	77	0.032
0.210	10	77	0.131
0.196	14	77	0.257
0.187	20	77	0.527



The low temperature energy bandgap of semiconductors vs their lattice constants



HgCdTe material system

HgCdTe is a nearly ideal infrared detector

Three key features:

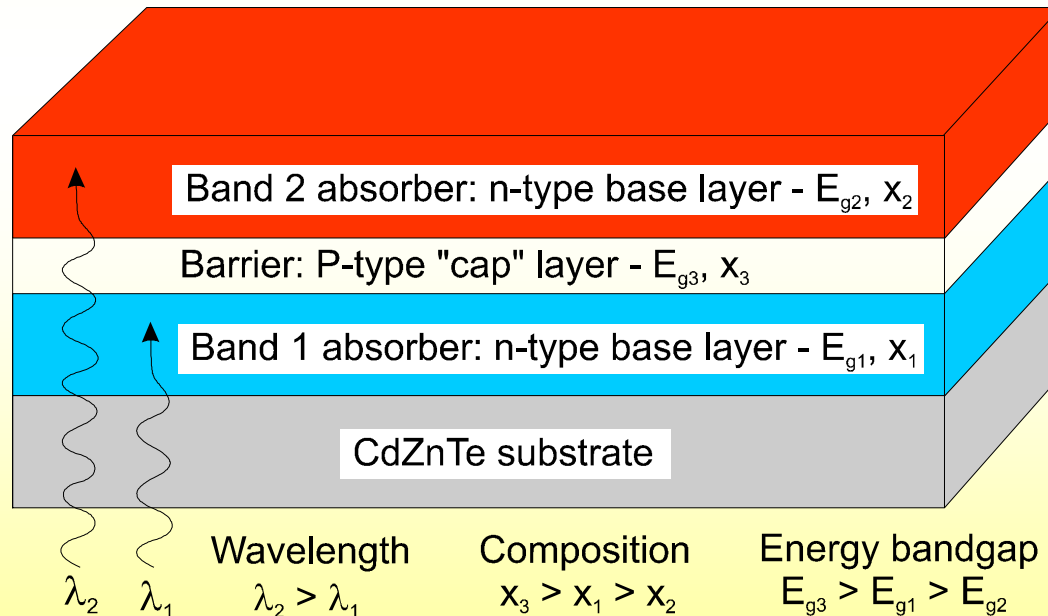
- tailorable energy band gap over the 1–30- μm range
- large optical coefficients that enable high quantum efficiency, and
- favorable inherent recombination mechanisms

The main motivations to replace HgCdTe:

- a weak Hg-Te bond, which results in bulk, surface and interface instabilities,
- uniformity and yield are still issues especially in the VLWIR spectral range.

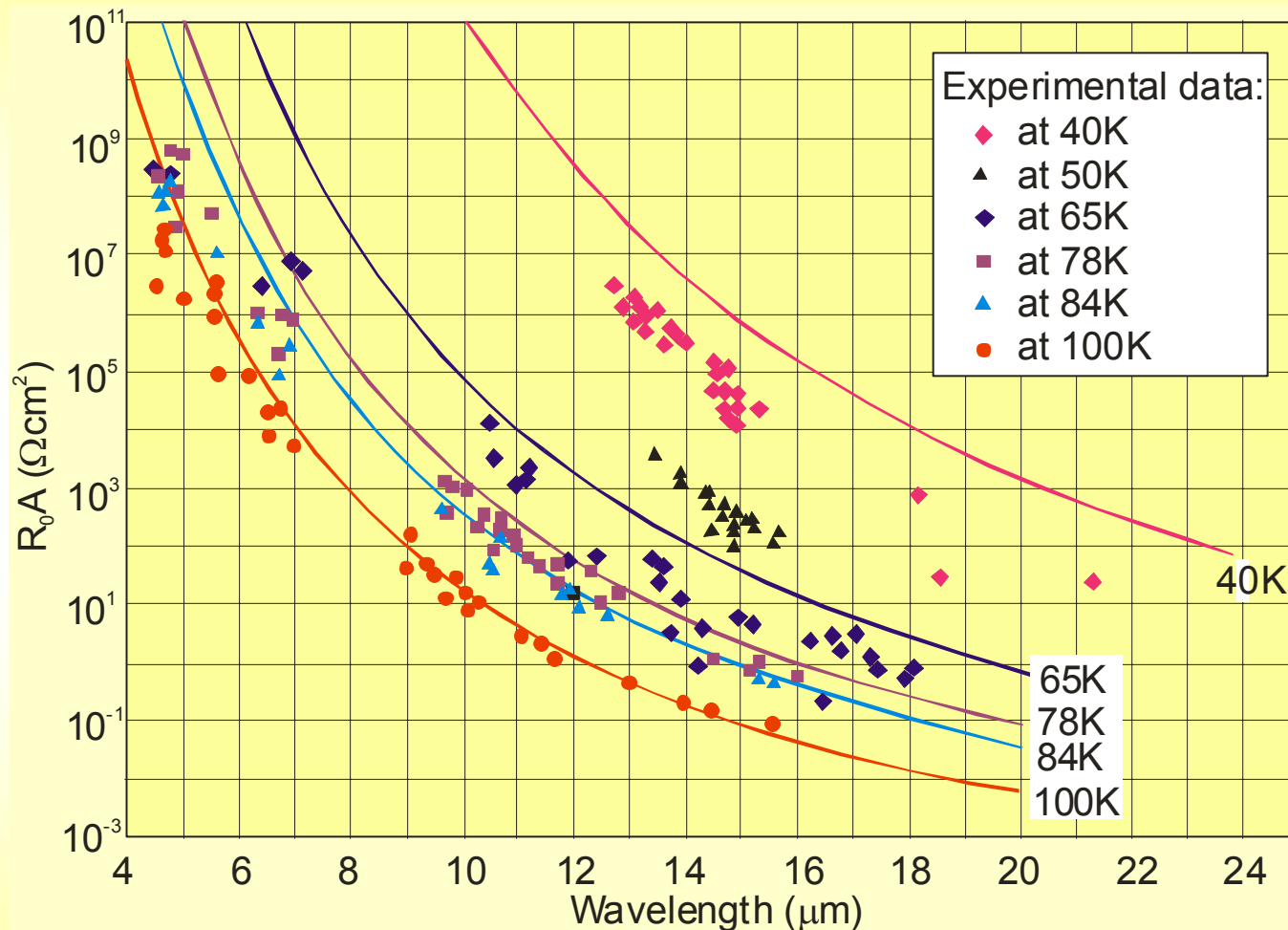
HgCdTe dual-band detectors

- Developed Raytheon, BAE, DRS, AIM, Rockwell and Leti
- Techniques: LPE, MOCVD and MBE
- A wide variety of pixel size (20 to 61 μm), array formats (64x64 up to 1280x720) and spectral-band sensitivity



Two color structure. Shorter wavelength flux is absorbed in Band 1, while longer wavelengths are absorbed in Band 2. A p-type layer forms a common contact

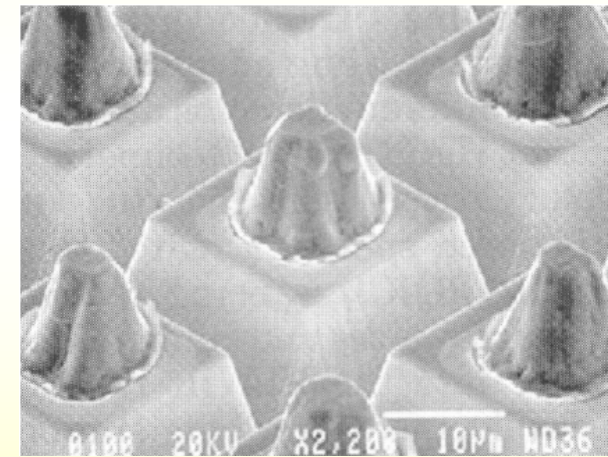
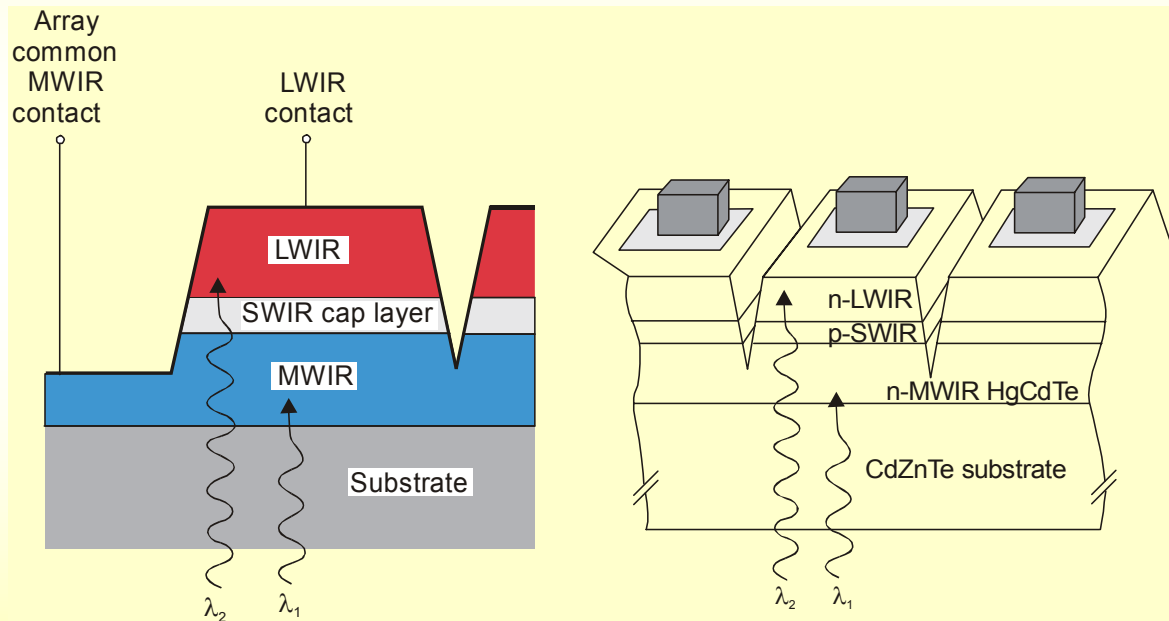
The separate photodiodes in a two-color detector perform exactly as single-color detectors in terms of achievable R_0A product



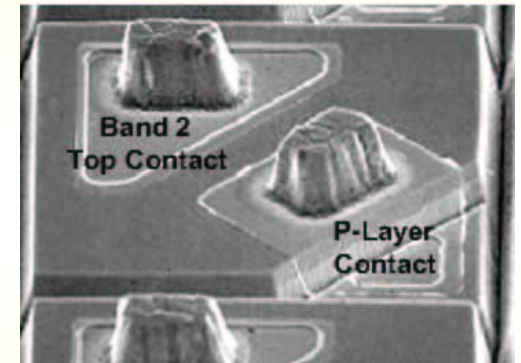
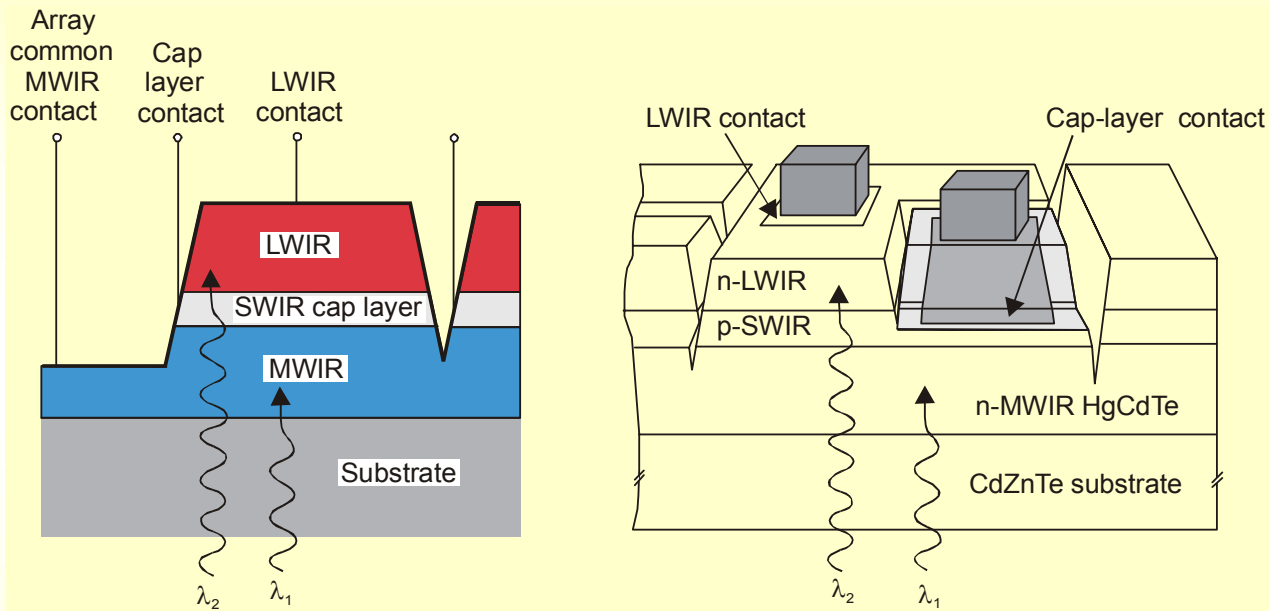
R_0A vs cutoff wavelength for RSC's HgCdTe photodiodes.
Experimental data are compared to theoretical best performance limit
[after T. Chuh, *Proc. SPIE* **5563**, 19-34 (2004)]

Sequential and simultaneous operation

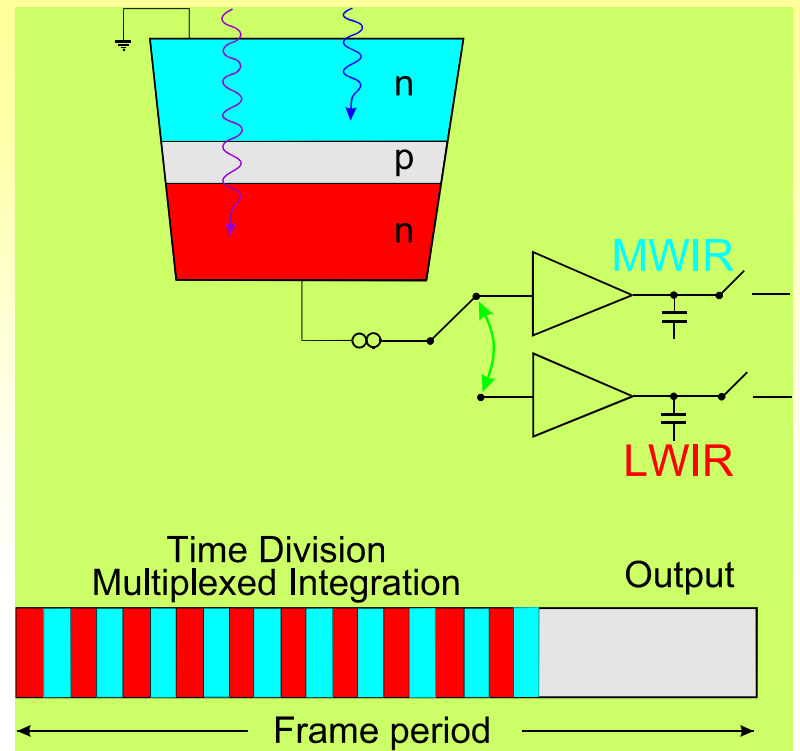
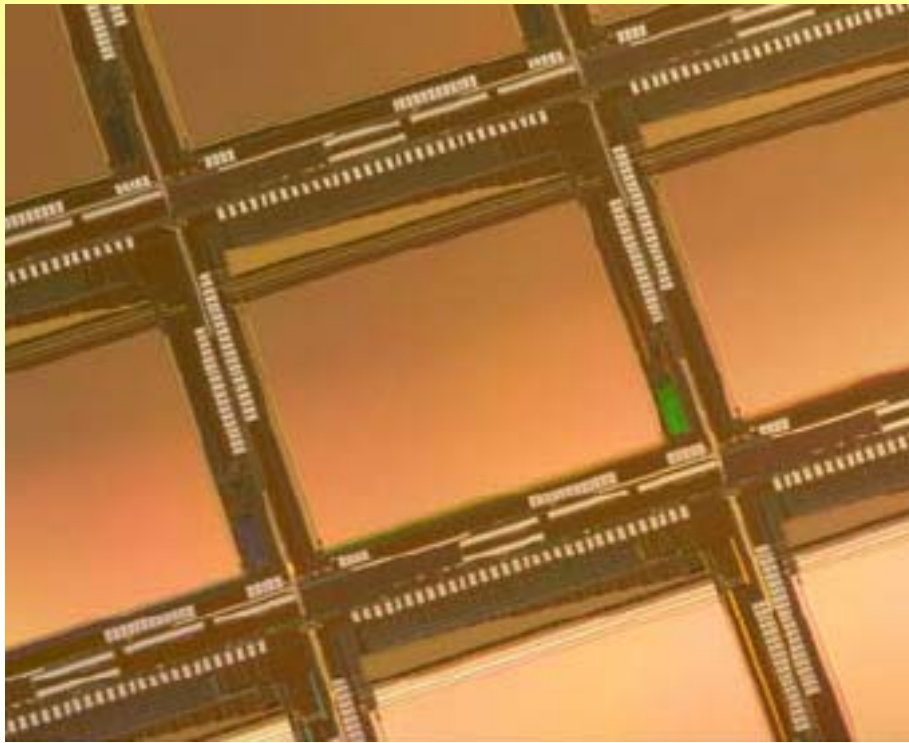
- Based upon an n-P-N HgCdTe TLHJ design
- The mode of detection is determined by the fabrication process



Cross section of integrated two-colour detectors
in an n-P-N layer structure for sequential operating mode



Cross section of integrated two-colour detectors in an n-P-N layer structure for simultaneous operating mode



Raytheon's two-color FPAs use a Time-Division-Multiplexed integration scheme:

- high fill factor - advantages over structures that require two contacts per unit cell
- detector current is directed to separate input circuitry and integration capacitors
- bias switching is performed at times much shorter than the frame time period (less than 1 ms)
- detector bias polarity is alternated many times within a single frame period

RVS has produced 640x480 two-colour FPAS with a 20- μm pixel pitch. Advanced FPA fabrication techniques such as inductively coupled plasma etching are being used to achieve benefits to detector performance.

NETDs less than 25 mK at f/5 have been demonstrated for both bands operating simultaneously

The 1280x720 two-color FPAs a 20- μm pixel pitch have demonstrated excellent sensitivity and pixel operabilities exceeding 99%.



(a) LWIR



(b) MWIR

Imagery obtained at 78K with f/2.8 field of view and 60 Hz frame rate using a two-colour 20- μm unit cell MW/LW HgCdTe/CdZnTe TLHJ 1280x720 IR FPA hybridized to a 1280x720 Time Division Multiplexed Integration ROIC [after E.P.G. Smith *et al.* *Proc. SPIE* **6127**, courtesy of RVS]



QWIPs

QWIP cannot compete with HgCdTe photodiode as the single device, especially at higher temperature operation (> 70 K) due to fundamental limitations associated with intersubband transitions

Parameter	HgCdTe	QWIP (n-type)	InAs/GaInSb SLS
IR absorption	Normal incidence	$E_{\text{optical}} \perp$ plane of well required Normal incidence: no absorption	Normal incidence
Quantum efficiency	$\geq 70\%$	$\leq 10\%$	$\approx 30\text{--}40\%$
Spectral sensitivity	Wide-band	Narrow-band (FWHM $\approx 1\text{--}2 \mu\text{m}$)	Wide-band
Optical gain	1	0.2-0.4 (30–50 wells)	1
Thermal generation lifetime	$\approx 1\mu\text{s}$	≈ 10 ps	$\approx 0.1\mu\text{s}$
R_0A product ($\lambda_c=10 \mu\text{m}$, $T=77\text{K}$)	$300 \Omega\text{cm}^2$	$10^4 \Omega\text{cm}^2$	$100 \Omega\text{cm}^2$
Detectivity ($\lambda_c=10 \mu\text{m}$, $\text{FOV}=0$)	$2 \times 10^{12} \text{ cmHz}^{1/2}\text{W}^{-1}$	$2 \times 10^{10} \text{ cmHz}^{1/2}\text{W}^{-1}$	$5 \times 10^{11} \text{ cmHz}^{1/2}\text{W}^{-1}$

- Even though QWIPs are photoconductors, several its properties such as high impedance, fast response time, and low power consumption comply well with the requirements for large FPAs fabrication
- The main drawbacks of LWIR QWIP FPA technology are the performance limitation for low integration time applications and low operating temperature
- Their main advantages are linked to performance uniformity, to availability of large size arrays, more thermal stability, and radiation hardness
- The large industrial infrastructure in III-V materials growth, processing, and packaging gives QWIPs a potential advantage in producibility and cost

State of the art QWIP and HgCdTe FPAs provide similar performance figure of merit, because they are predominantly limited by the readout circuits

For charge-limited HgCdTe photodiodes

$$NEDT = \frac{2kT_B^2\bar{\lambda}}{hc\sqrt{2N_w}}$$

For storage capacity of 2×10^7 electrons, $\lambda = 10 \mu\text{m}$, and $T_B = 300 \text{ K}$, $NEDT = 19.8 \text{ mK}$. The same estimation for QWIP gives

$$NEDT = \frac{2kT_B^2\bar{\lambda}}{hc} \sqrt{\frac{g}{N_w}}$$

The value of $NEDT$ in a charge-limited QWIP detectors is better than that of HgCdTe photodiodes by a factor of $(2g)^{1/2}$ since a reasonable value of g is 0.4. Assuming the same operation conditions as for HgCdTe photodiodes, the value of $NEDT$ is 17.7 mK.

A low photoconductive gain actually increases the S/N ratio and a QWIP FPA can have a better $NEDT$ than an HgCdTe FPA with a similar storage capacity.

The very short integration time of LWIR HgCdTe devices of typically below $300 \mu\text{s}$ is very useful to freeze a scene with rapidly moving objects. For QWIP devices however, the integration time must be 10 to 100 times longer and typically is 5–20 ms.

(a)



(b)



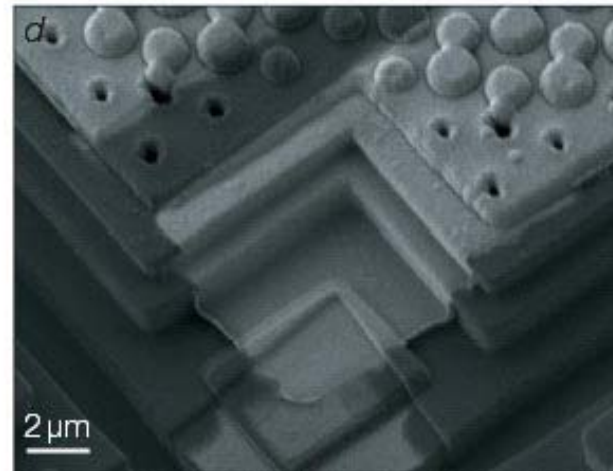
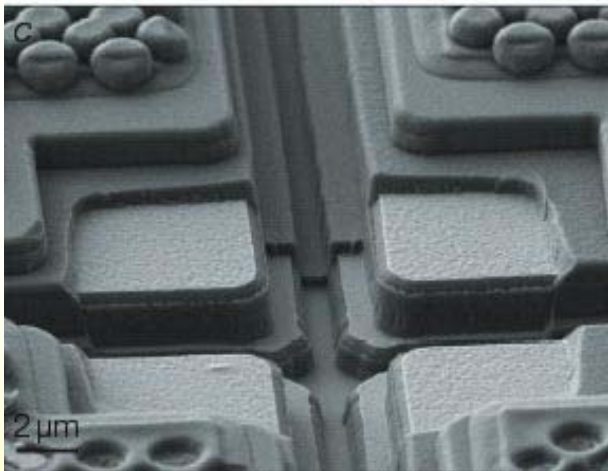
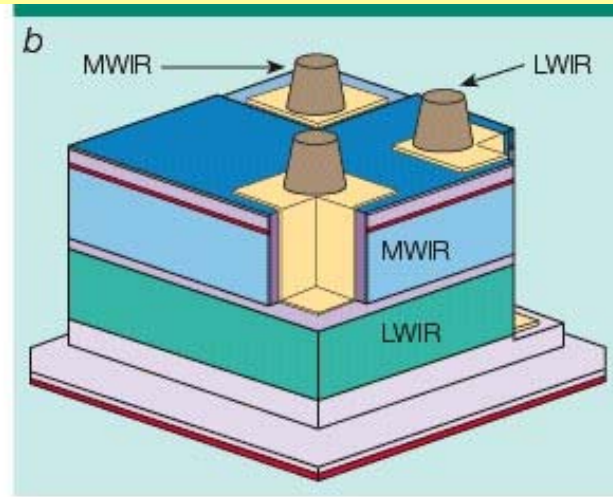
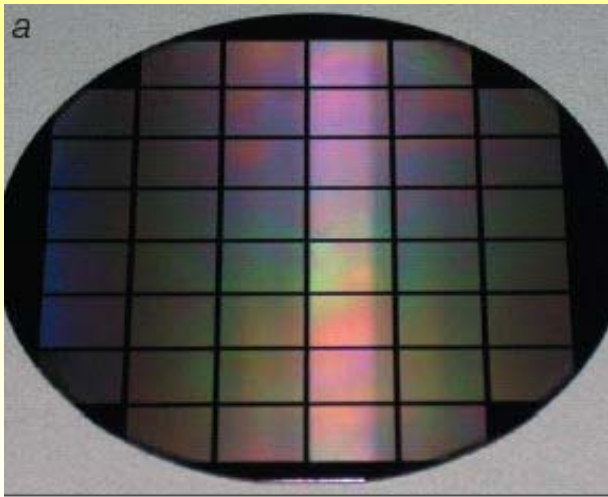
1 megapixel hybrid MWIR and LWIR QWIPs with 18- μm pixel size have been demonstrated:

- the MWIR array: $NEDT = 17$ mK at 95K (f/2.5 optics, 300 K background)
- the LWIR array: $NEDT = 13$ mK at 70K (f/2.5 optics, 300 K background)

This technology can be extended to a 2K \times 2K array, but at present the limitation is the readout availability and cost

[after S.D. Gunapala *et al.*,
Semicond. Sci. Technol. **20**, 473–480 (2005)]

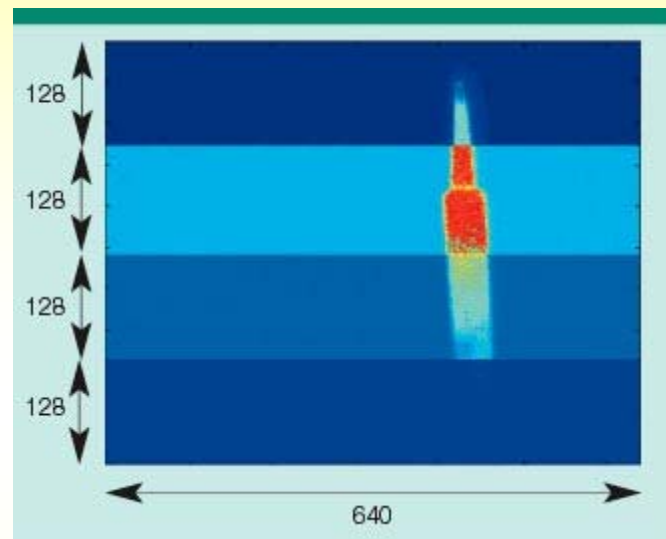
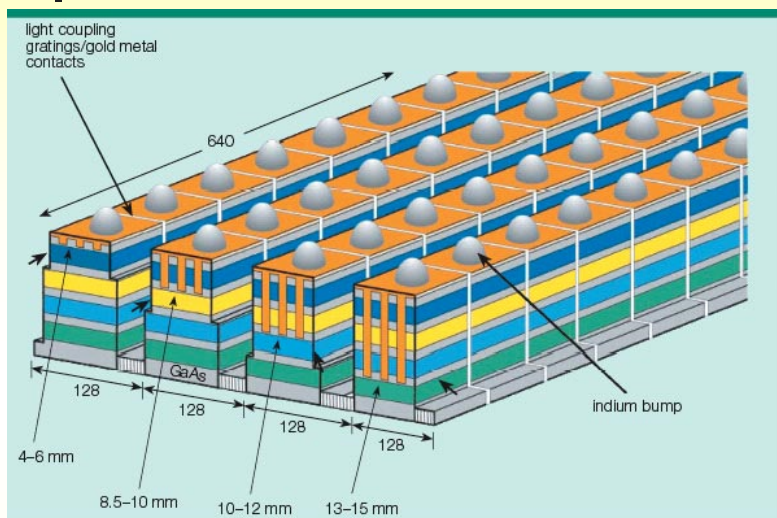
One frame of video image taken with the 5.1 μm (a) and 9 μm (b) cutoff 1024x1024 pixel QWIP camera



JPL has used 4 inch wafers to fabricate dual-band QWIP devices

(after S.D. Gunapala, *Compound Semiconductor*, October 2005)

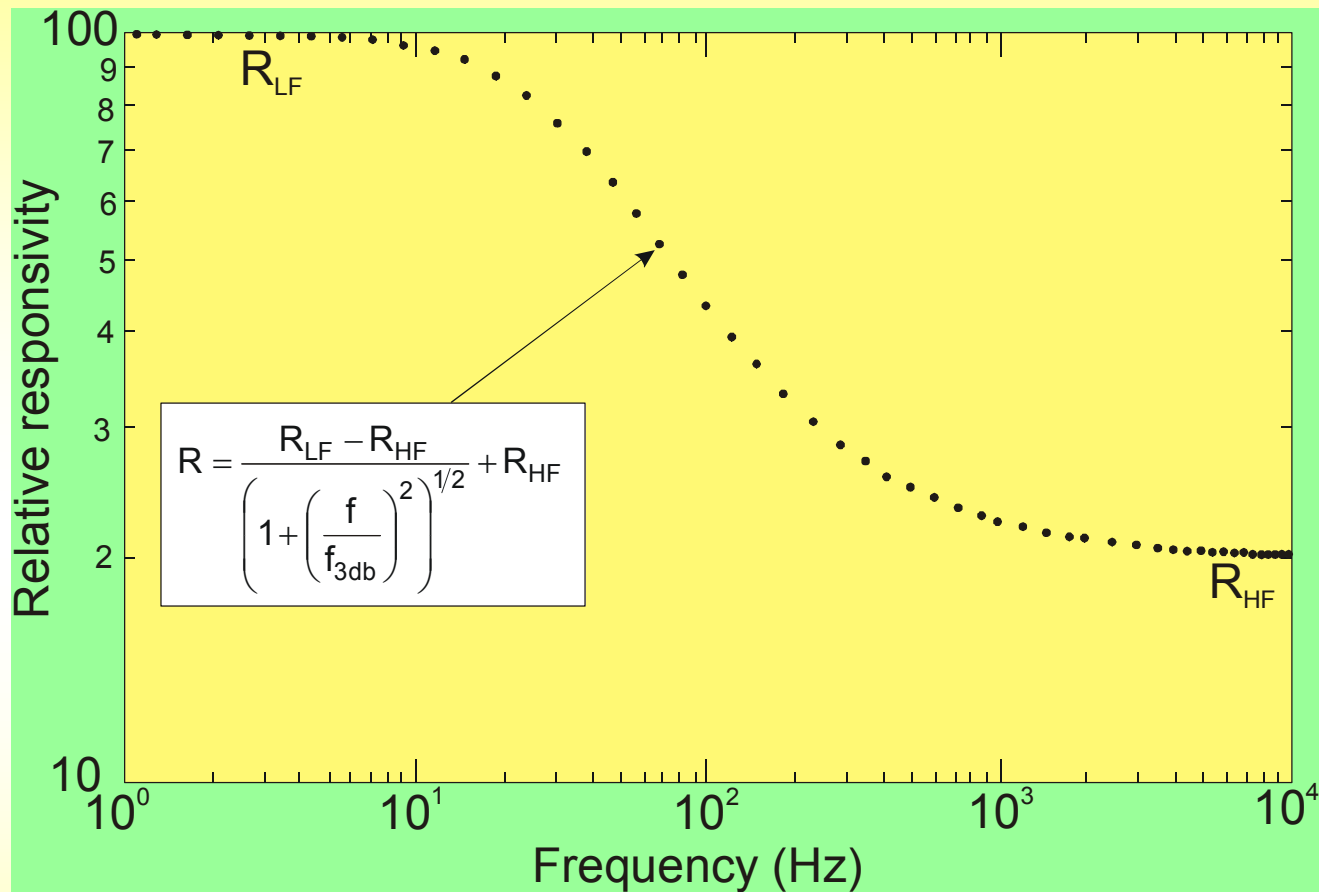
QWIPs – four colour arrays



after S.D. Gunapala *et al.*, *IEEE Trans. Electron Devices* **50**, 2353–2360 (2004)

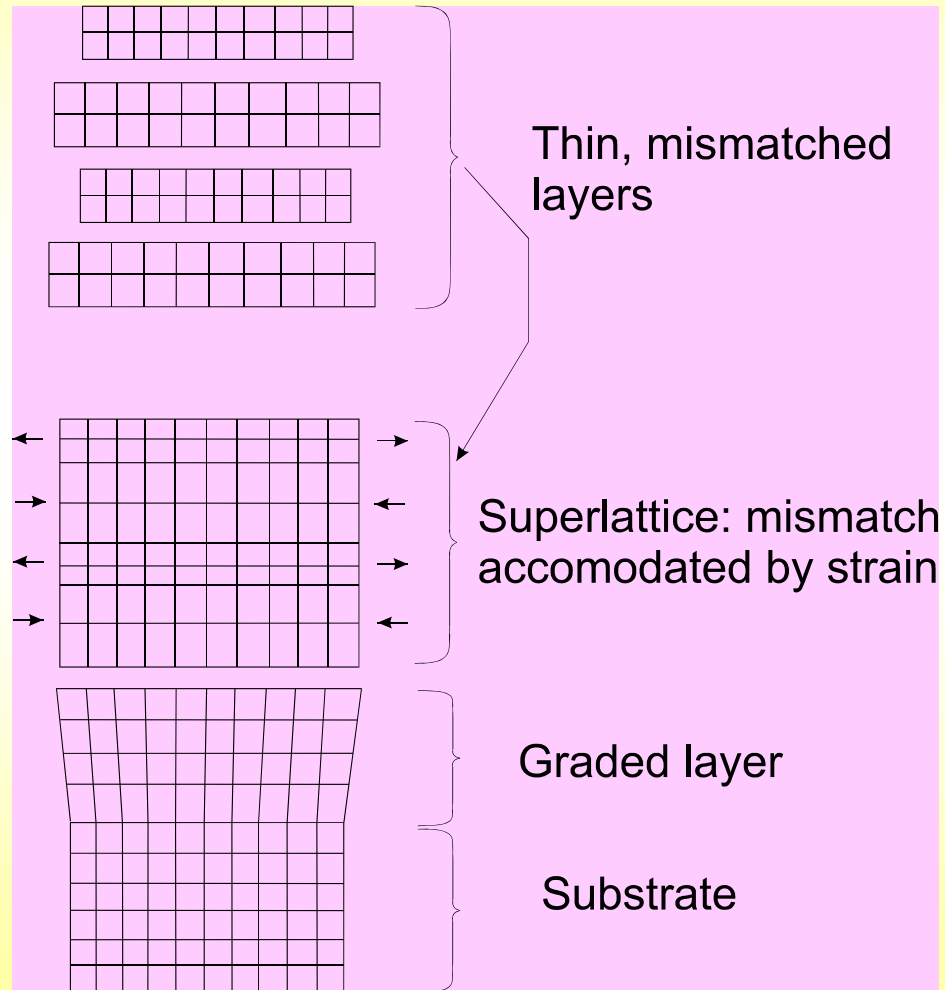
The 640×512 format FPA consists of four 640×128 pixel areas which are capable of acquiring images in these bands.

Four separate detector bands were defined by a deep trench etch process and the unwanted spectral bands were eliminated by a detector short-circuiting process



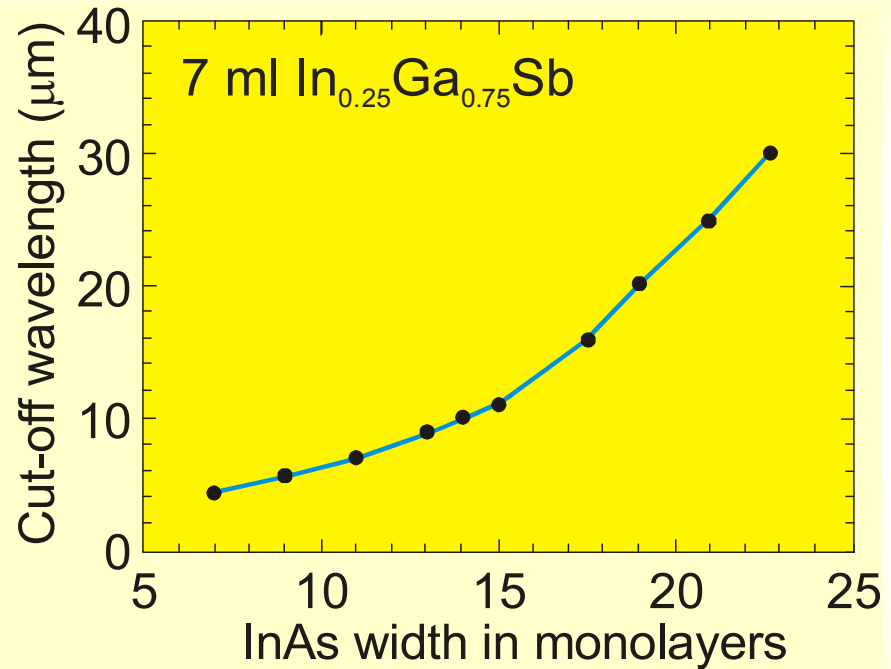
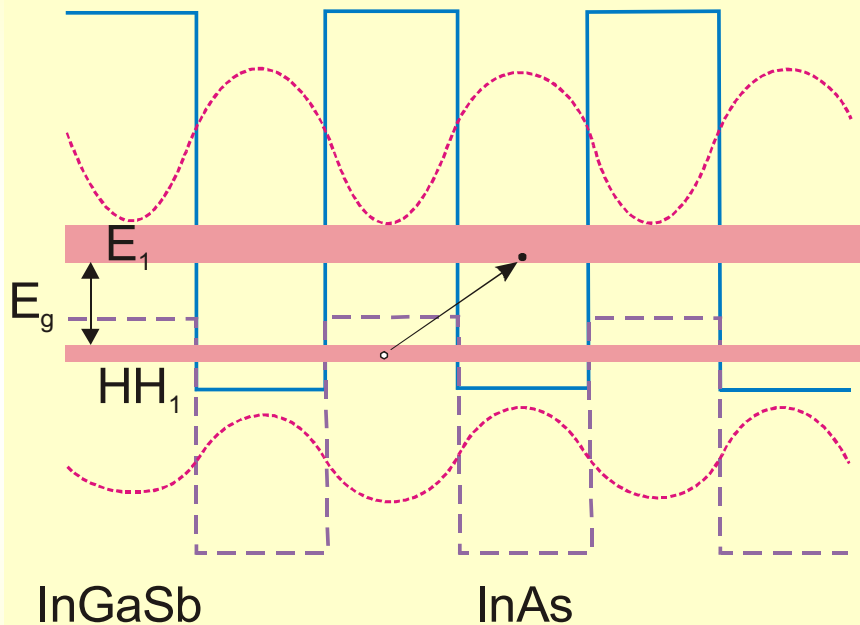
QWIP devices are not suitable for space based remote sensing applications operation due to dielectric relaxation effects and flux memory effects
 [after D.C. Arrington *et al.*, *Proc. SPIE 4028*, 289–299 (2000)]

InAs/Ga_{1-x}In_xSb SLSs



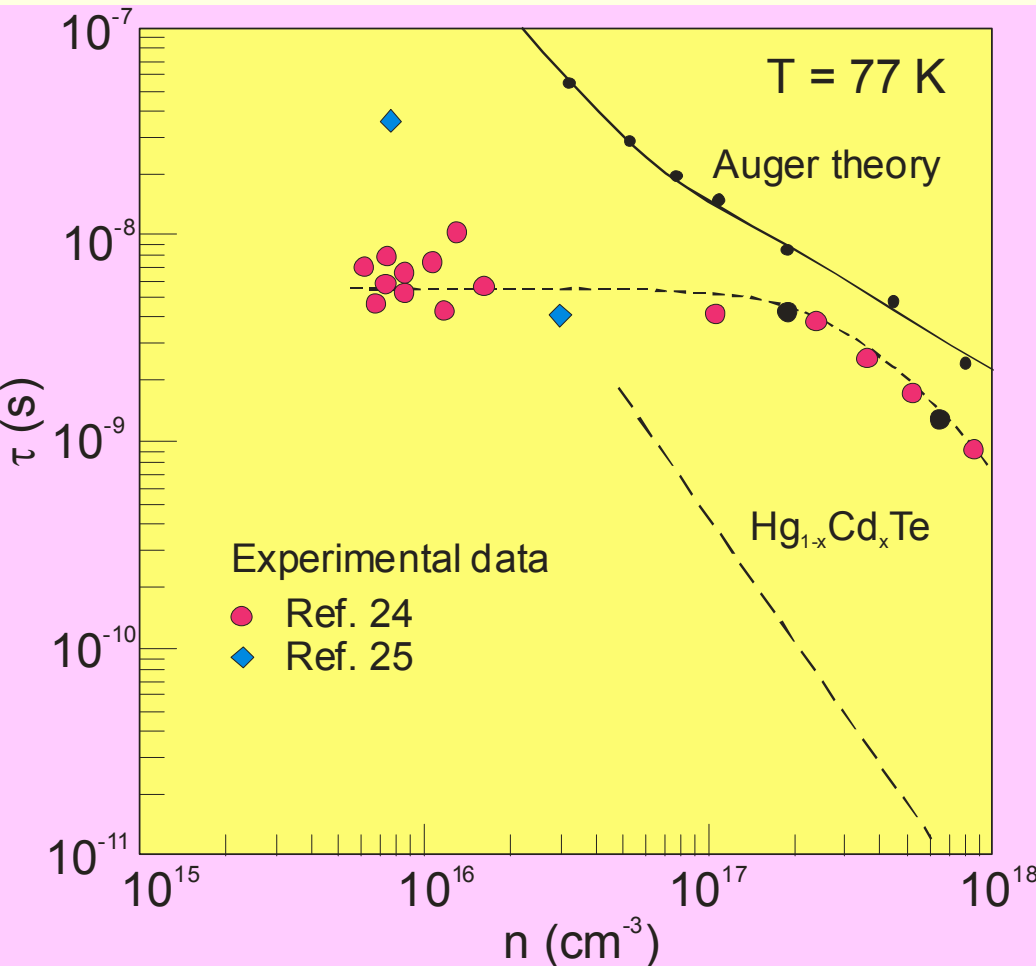
Schematic of strained layer superlattice

InAs/Ga_{1-x}In_xSb SLSs



InAs/GaInSb strained layer superlattice: (a) band edge diagram illustrating the confined electron and hole minibands which form the energy band gap; (b) change in cut-off wavelength with change in one superlattice parameter – InAs layer width [after G.J. Brown *et al.*, *Proc. SPIE 4999*, 457–466 (2003)]

- Theoretically, InAs/Ga_{1-x}In_xSb SLS have some advantages over bulk HgCdTe, including lower leakage currents and greater uniformity [D.L. Smith and C. Mailhot, *J. Appl. Phys.* **62**, 2545–2548 (1987)]
- High performance InAs/GaInSb SL photodiodes was predicted by the theoretical promise of longer intrinsic lifetimes due to the suppression of Auger recombination mechanism



Comparison of measured and calculated carrier lifetimes of InAs/GaInSb SLS (about 120 eV energy gap) at 77 K as a function of carrier density

Experimental data:

(●) after E.R. Youngdale *et al.*, *Appl. Phys. Lett.* **64**, 3160 (1994)

(◆) after O.K. Yang *et al.*, *Proc. SPIE* **4999**, 448 (2003)

Theory:

(●) after E.R. Youngdale *et al.*, *Appl. Phys. Lett.* **64**, 3160 (1994)

Detectivity

$$D^* = 0.31 \frac{\lambda}{hc} k \left(\frac{\alpha}{G} \right)^{1/2}$$

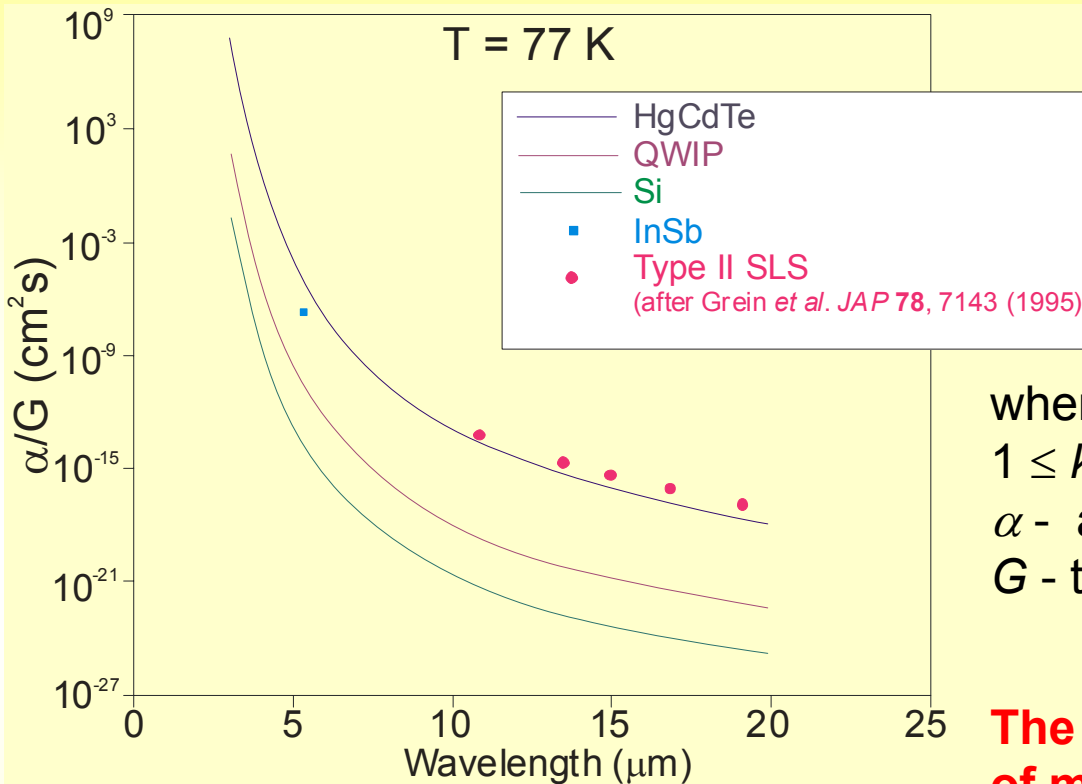
where

$$1 \leq k \leq 2$$

α - absorption coefficient

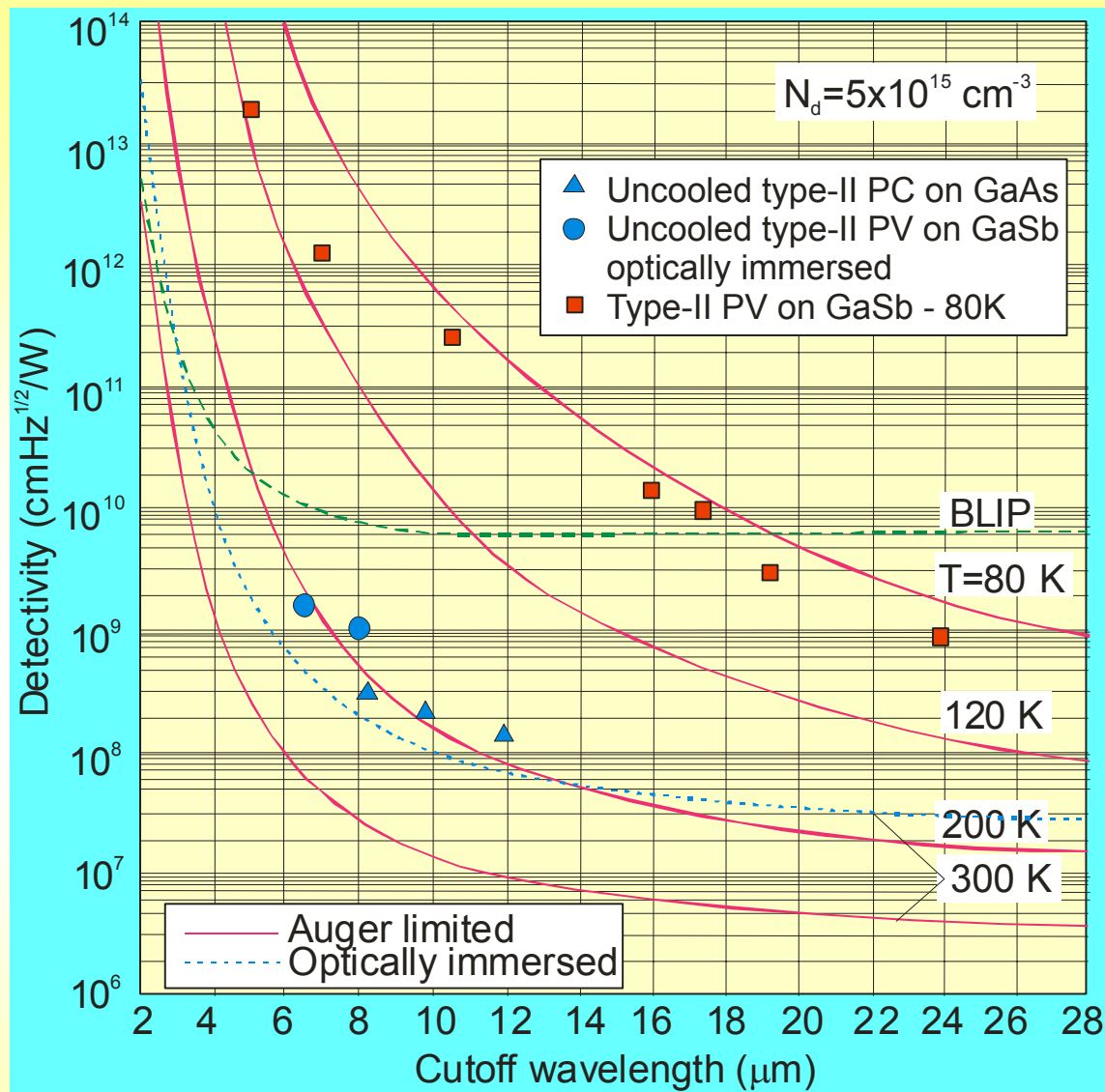
G - thermal generation

The ratio α/G is the fundamental figure of merit of any material for IR photodetectors



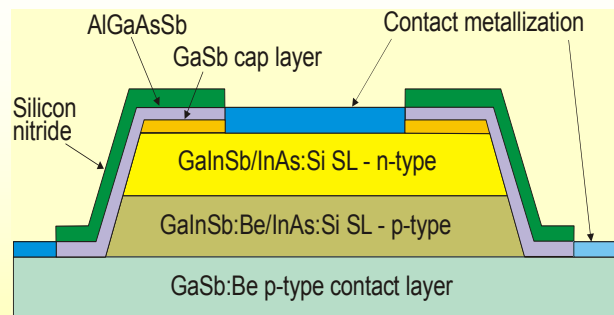
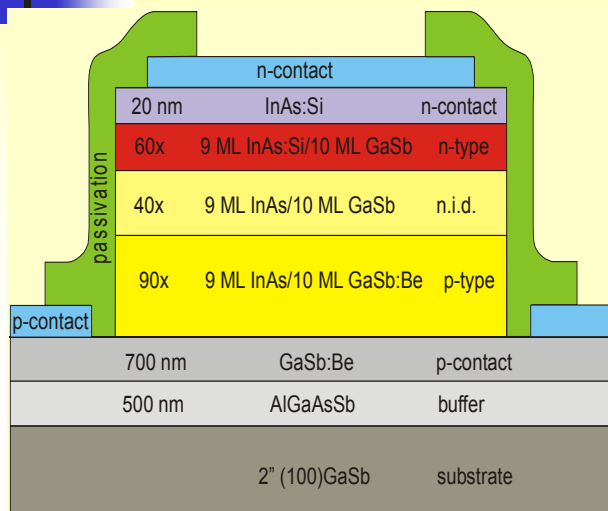
SL material issues:

- residual doping of the order of $5 \times 10^{15} \text{ cm}^{-3}$,
- Shockley-Read limited lifetime at lower temperature (< 77 K).



Calculated performance of Auger generation-recombination limited HgCdTe photodetectors compared to type II superlattice experimental data from Center for Quantum Devices, Northwestern University

Photodiode configurations



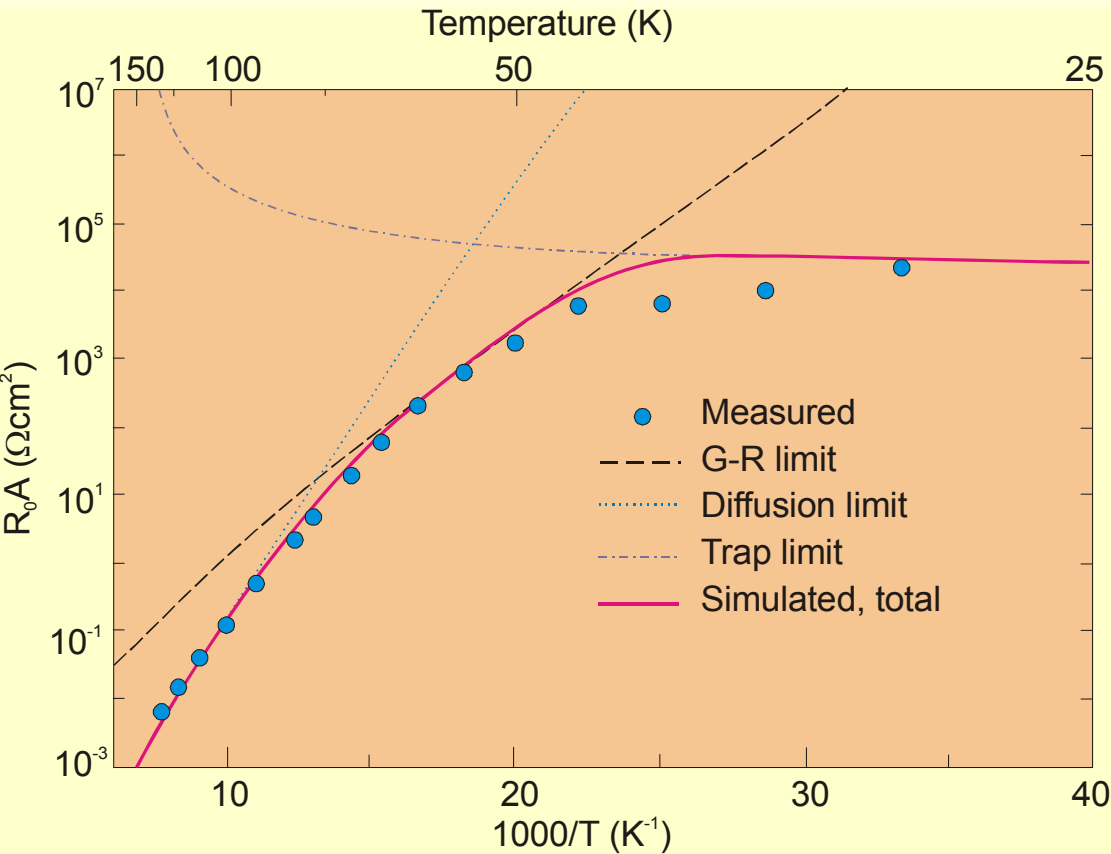
- Superlattice photodiodes are based p-i-n structures with an unintentionally doped, intrinsic region between the heavily doped contact portions of the device
- InAs/GaInSb LWIR photodiodes are fabricated with the In molar fraction in the GaInSb layers close to 20%
- Optimization of the SL photodiode architectures is still an open area

Cross section schematic of p-i-n SL photodiodes for the MWIR and LWIR

[after R. Rehm *et al.*, *Proc. SPIE* **5783**, 123–130 (2005)]

Performance:

- depletion region limited in temperature range $50\text{K} \leq T \leq 80\text{K}$,
- trap-assisted tunnelling at low temperature $< 50\text{ K}$ (trap density $1 \times 10^{12}\text{ cm}^{-3}$),
- R_0A exceeding $100\ \Omega\text{cm}^2$ even with $\lambda_c \approx 14\ \mu\text{m}$ can be achieved.



Experimental data and theoretical prediction of the R_0A product as a function of temperature:

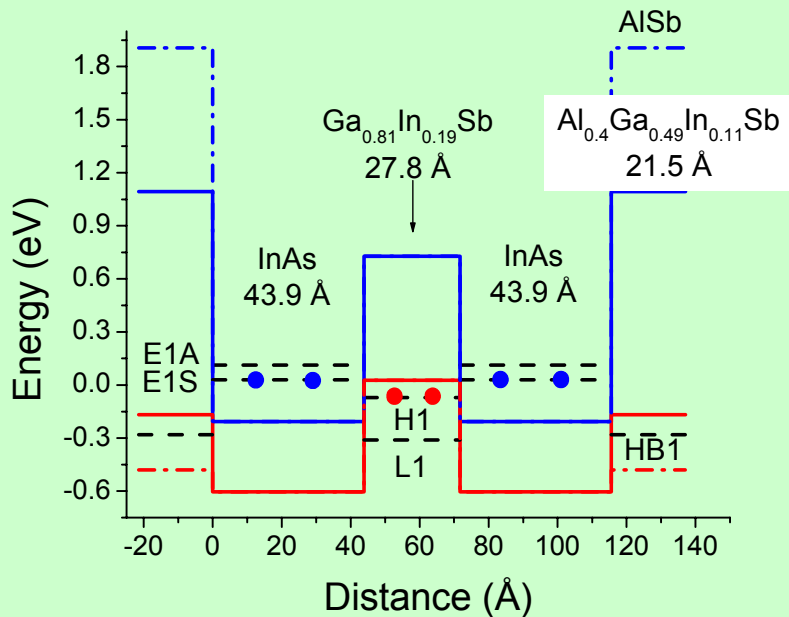
$$\lambda_c = 11\ \mu\text{m}$$

$$\text{trap density} = 1 \times 10^{12}\ \text{cm}^{-3}$$

[after O.K. Yang et al., *Proc. SPIE* **4999**, 448–456 (2003)]

W-structured type II SL LWIR photodiodes

R_0A values comparable for state-of-the-art HgCdTe

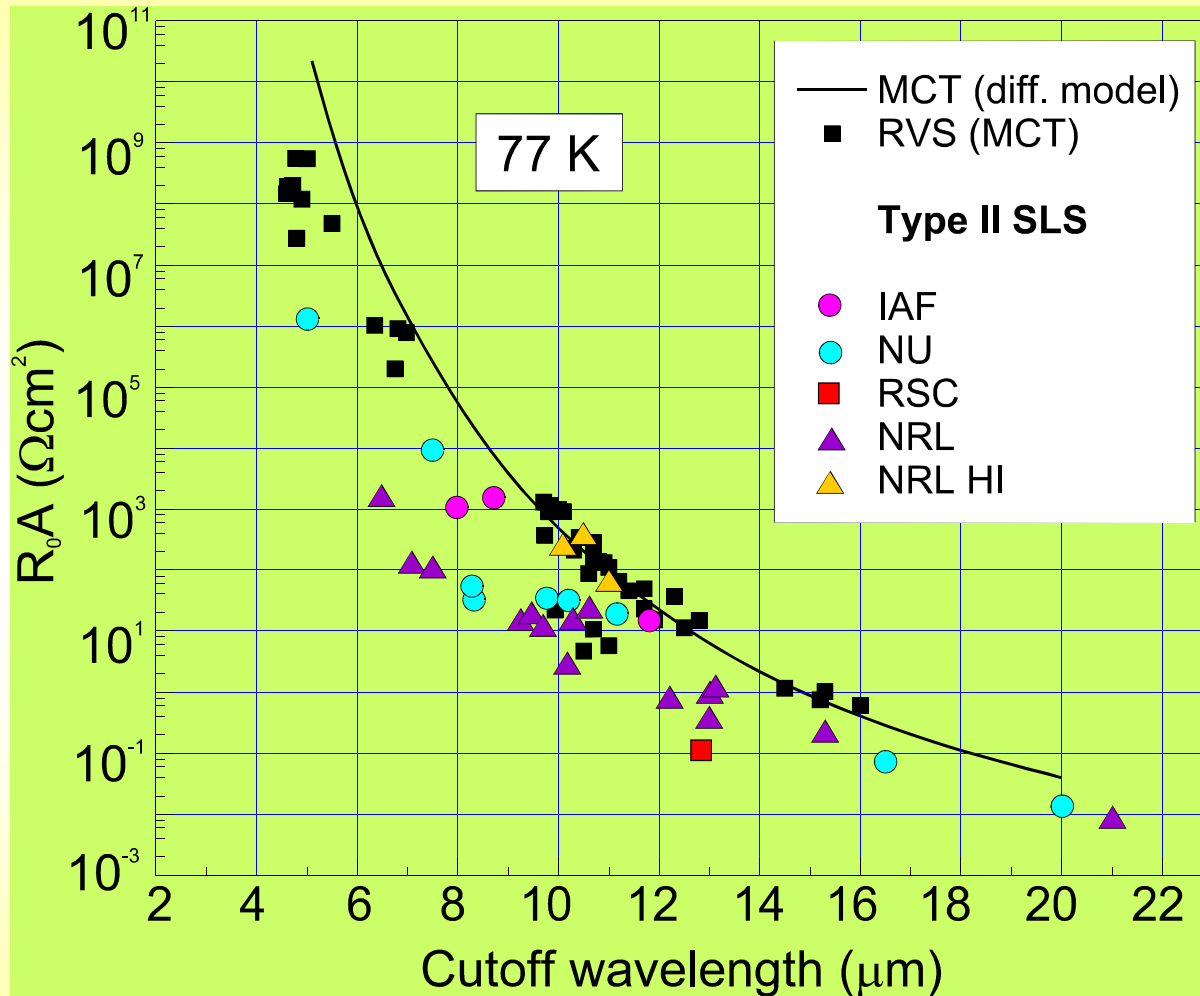


- two InAs "electron-wells" are located on either side of an InGaSb "hole-well" and are bound on either side by AlGaInSb "barrier" layers
- $R_0A = 174 \Omega\text{cm}^2$ at 80 K, and excess of $300 \Omega\text{cm}^2$ at 77 K, for devices with a $10.5 \mu\text{m}$ cutoff wavelength

High quantum efficiency WSL used for
"i-region" absorber layer

[after E.H. Aifer *et al.*, to be published]

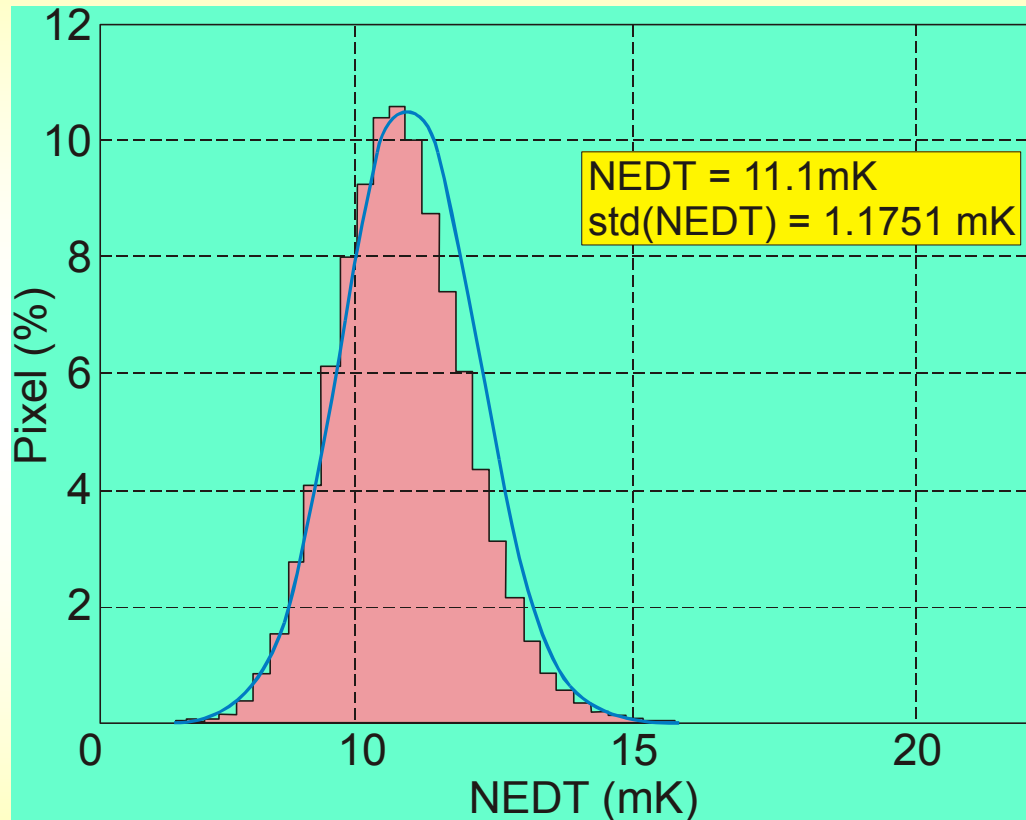
Results for SLS devices rival that of practical HgCdTe devices



Dependence of the R_0A product of InAs/GaInSb SLS photodiodes on cutoff wavelength compared to theoretical and experimental trendlines for comparable HgCdTe photodiodes at 77 K (after E.H. Aifer *et al.*, to be published)

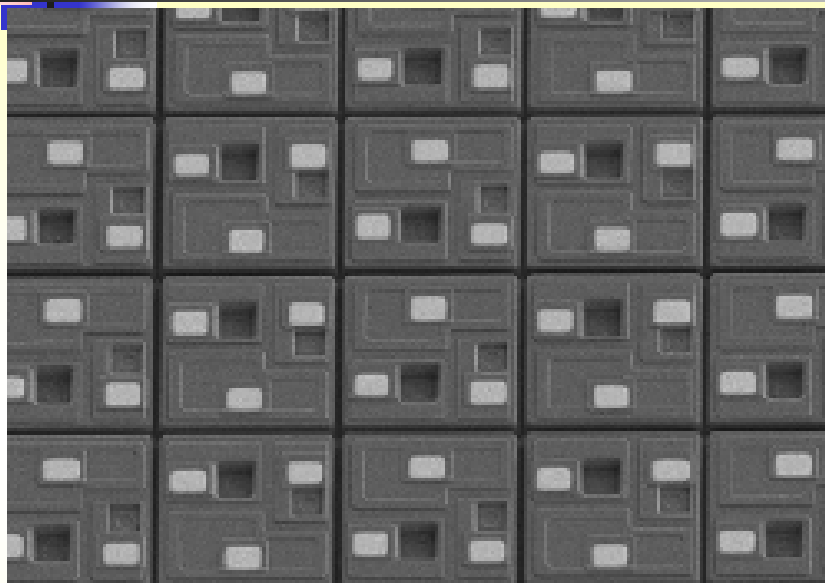
256×256 FPAs (Fraunhofer Institut, Freiburg)

$\lambda_c \approx 5.3 \mu\text{m}$ and $10.4 \mu\text{m}$, pitch $40 \mu\text{m}$, $A_{ph} = 38 \times 38 \mu\text{m}^2$

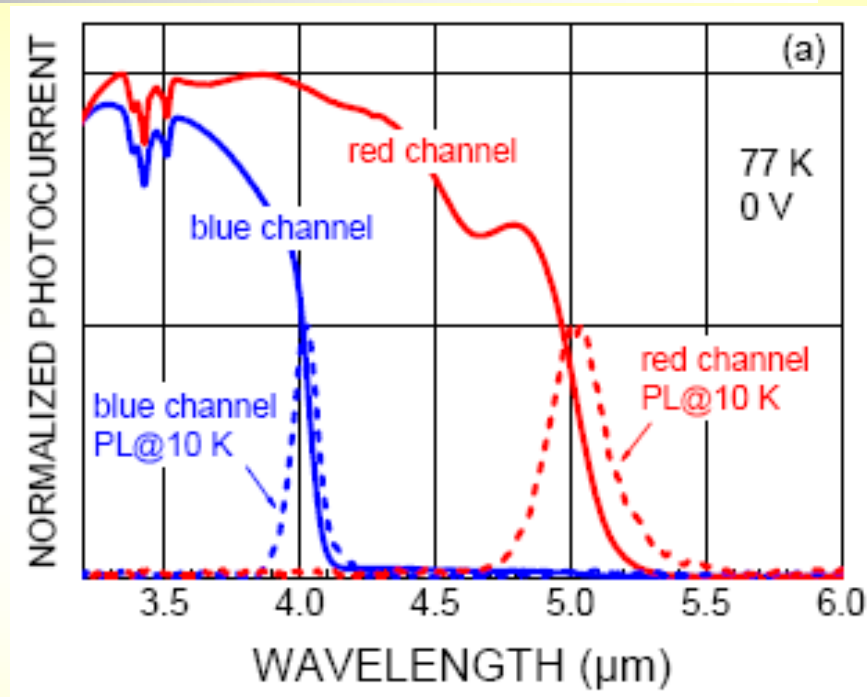


NEDT of a 256×256 MWIR InAs/GaInSb superlattice FPA
($\lambda_c = 5.3 \mu\text{m}$, $f/2$ optics, $t_{int} = 5 \text{ ms}$)
(after M. Münzberg *at el.*)

First type II dual-colour detector



(a)

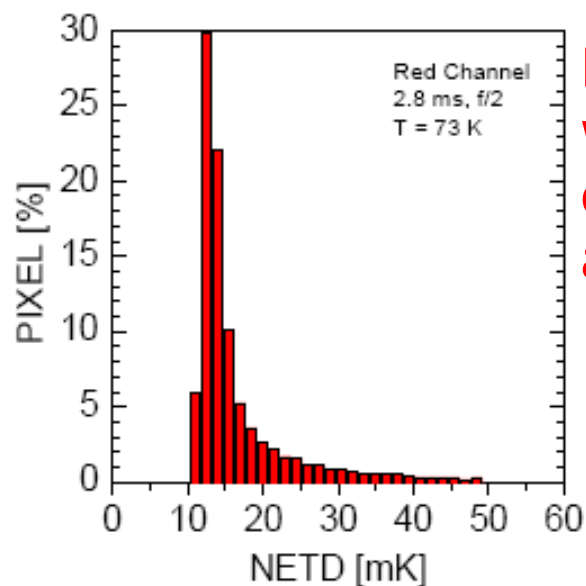
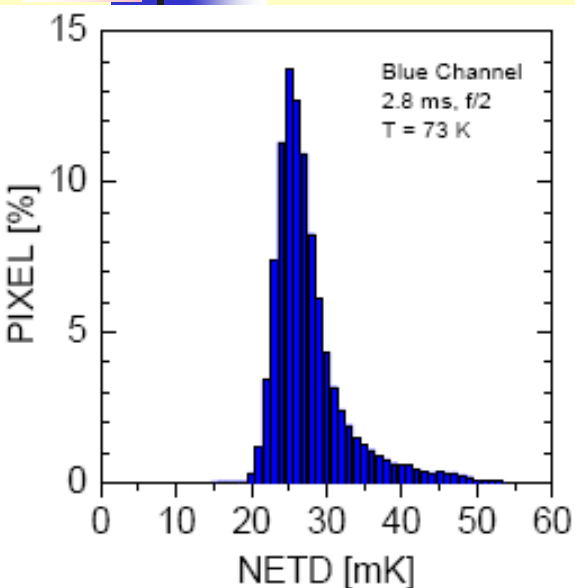


(b)

288x384 dual-colour 20- μm unit cell MW InAs/GaSb SL-FPAs: (a) SEM image, (b) normalized photocurrent at 77 K and photoluminescence signal at 10 K [after R. Rehm et al., *Proc. SPIE* **6206**, 62060Y (2006)].

The thickness of the detector is only 4.5 μm , which significantly reduces the technological challenge compared to bispectral HgCdTe detector with a typical layer thickness around 15 μm

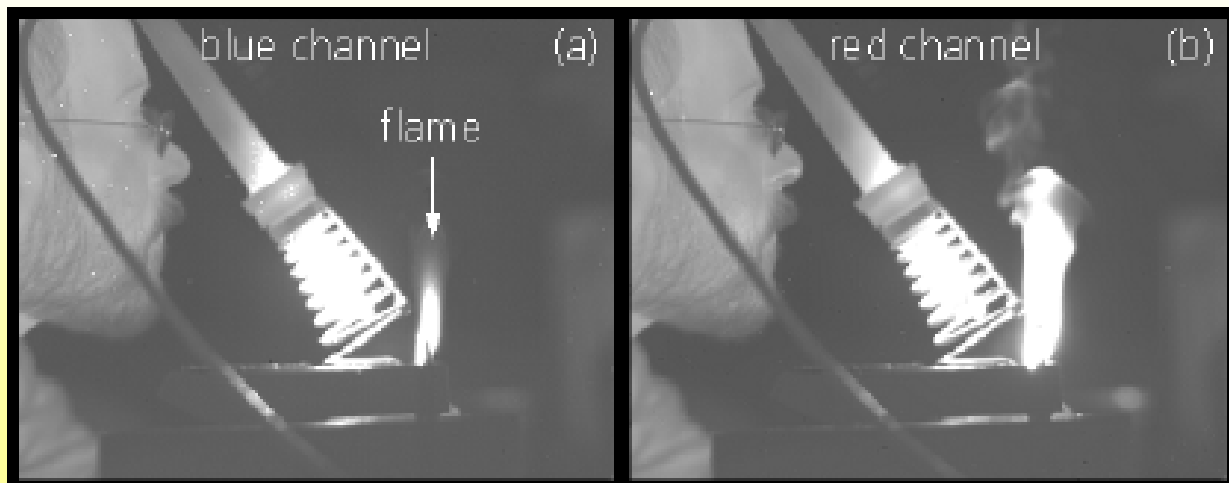
Electro-optical characterization



NETD histogram data at 73 K with f/2 optics and $\tau_{\text{int}}=2.8$ ms of the blue ($3.4 \leq \lambda \leq 4.1 \mu\text{m}$) and red channel ($4.1 \leq \lambda \leq 5.1 \mu\text{m}$)

Simultaneous mode of operation

Imagers delivered by the 288x384 dual-colour InAs/GaSb camera





Conclusions

- Third generation infrared imagers are beginning a challenging road to deployment
- It is predicted that HgCdTe technology will continue in the future to expand the envelope of its capabilities because of its excellent properties.
- Despite serious competition from alternative technologies and slower progress than expected, HgCdTe is unlikely to be seriously challenged for high-performance applications, applications requiring multispectral capability and fast response in the SWIR, MWIR and LWIR spectral regions
- Nonuniformity is a serious problem in the case of VLWIR HgCdTe detectors. For applications that require operation in the VLWIR band as well as two-color LWIR/VLWIR bands most probably HgCdTe will not be the optimal solution



Conclusions

- Based on the breakthrough of Sb-based type II SLS technology it is obvious that this material system is in position to provide high thermal resolution for short integration times comparable to HgCdTe.
- Fact that Sb-based superlattices are processed close to standard III-V technology the potential to be more competitive due to lower costs in production
- Type II InAs/GaInSb SL structure is a relatively new alternative IR material system and has great potential for LWIR/VLWIR spectral ranges with performance comparable to HgCdTe with the same cutoff wavelength
- Type II InAs/GaInSb material system is also very promising for uncooled LWIR applications



Thank you